Brief Definitive Report

The CCR7 Ligand ELC (CCL19) Is Transcytosed in High Endothelial Venules and Mediates T Cell Recruitment

By Espen S. Baekkevold,* Takeshi Yamanaka,* Roger T. Palframan,§
Hege S. Carlsen,* Finn P. Reinholt,‡ Ulrich H. von Andrian,§
Per Brandtzaeg,* and Guttorm Haraldsen*

From the *Laboratory for Immunohistochemistry and Immunopathology (LIIPAT) and the
‡Laboratory for Electron Microscopy, Institute of Pathology, University of Oslo, Rikshospitalet,
N-0027 Oslo, Norway; and §The Center for Blood Research, Department of Pathology,
Harvard Medical School, Boston, Massachusetts 02115

Abstract

Lymphocyte homing to secondary lymphoid tissue is defined by a multistep sequence of interactions between lymphocytes and endothelial cells in high endothelial venules (HEVs). After initial selectin-mediated tethering and rolling, firm adhesion of lymphocytes requires rapid upregulation of lymphocyte integrin adhesiveness. This step is mediated in part by the HEV-derived chemokine SLC (secondary lymphoid-tissue chemokine, or CCL21) that binds to the CC chemokine receptor (CCR)7 on lymphocytes. However, the CC chemokine ELC (Epstein-Barr virus–induced molecule 1 ligand chemokine, or CCL19) shares the same receptor, and ELC transcripts have been observed in the T cell areas of lymphoid organs. Here, we show that perivascular ELC is transcytosed to the luminal surfaces of HEVs and enables efficient T cell homing to lymph nodes. In situ hybridization on sections of human tonsil showed no ELC mRNA in HEVs, but immunostaining revealed ELC protein in cytoplasmic vesicles of HEV cells. Furthermore, ELC injected into the footpads of mice entered the draining lymph nodes and was presented by HEVs. Finally, intracutaneous injections of ELC in mice lacking functionally relevant ELC and SLC (plt/plt mice) restored T cell trafficking to draining lymph nodes as efficiently as SLC. We conclude that perivascular ELC is transcytosed to the luminal surfaces of HEVs and participates in CCR7-mediated triggering of lymphocyte arrest.

Key words: chemokines • lymphocyte trafficking • vascular endothelium • lymphoid tissue • plt/plt mice

Introduction

Continuous migration of lymphocytes from the peripheral blood to organized lymphoid tissue and back to the circulation is essential for immune surveillance and the generation of immune responses. Lymphocyte emigration in peripheral lymphoid organs occurs through the walls of high endothelial venules (HEVs) in a stepwise sequence of interactions between lymphocytes and HEV cells (1–3). This adhesion cascade is initiated by selectin-mediated rolling but requires a subsequent signaling event that triggers rapid integrin–mediated adhesion to the endothelium, and finally diapedesis. Recently, several candidate chemotactic cytokines (chemokines) with a potential to induce such lymphocyte triggering under flow conditions have been identified

(4). These include chemokines constitutively expressed in lymphoid tissue (and thus termed "lymphoid chemokines"), such as SLC (secondary lymphoid-tissue chemokine, also called 6Ckine, exodus 2, or TCA-4, and recently designated CCL21) and ELC (Epstein-Barr virus–induced molecule 1 ligand chemokine, also called macrophage inflammatory protein (MIP)-3β, exodus 3, or CCL19) (5–7). SLC and its receptor, CCR7, are currently regarded as the best candidates for chemokine-induced adhesion triggering in HEVs. Thus, SLC is expressed by HEV endothelium in normal mice (8–10) but is lacking in mice homozygous for a spontaneous mutation, plt (paucity of lymph node T cells), that have severe defects in T cell homing (9–13). Furthermore, chemokine-induced desensitization of CCR7 inhibits T cell adherence to HEVs in wild-type mice (9, 10). Moreover, mice with targeted deletion of the SLC receptor CCR7 have severe defects in lymphocyte homing to peripheral lymphoid organs (14). On the other

E.S. Baekkevold and T. Yamanaka contributed equally to this work.
   Address correspondence to Espen S. Baekkevold, LIIPAT, Rikshospitalet, N-0027 Oslo, Norway. Phone: 47-2307-1494; Fax: 47-2307-1511; E-mail: e.s.bakkevold@labmed.uio.no

hand, a role for ELC in triggering of shear-resistant lymphocyte adhesion to the HEV surface has been less obvious. Although ELC shares with SLC the binding specificity to CCR7, attracts the same major populations of lymphocytes (15, 16), and has recently been shown to be deleted in *plt/plt* mice as well (17, 18), ELC transcripts are restricted to nonendothelial cells in the T cell zone of secondary lymphoid organs (19, 20). However, abluminal internalization and subsequent transcytosis of chemokines can apparently take place in endothelial cells, because intradermally injected IL-8 (CXCL8) was shown to be transendothelially transported and luminally posted in postcapillary venules (21). In this manner, perivascular expression of chemokines may be relayed to circulating leukocytes.

Here we show that perivascular ELC is taken up by HEV cells and translocated to their luminal surface membranes. In situ mRNA hybridization performed on sections of human tonsils demonstrated strong mRNA signals from cells in the T cell zone, but no transcripts were detected in HEVs. However, immunohistochemical staining revealed ELC in cytoplasmic vesicles of HEV cells as well as in perivascular cells. Furthermore, ^{125}I–ELC injected into footpads of mice entered draining lymph nodes and was detected in HEV cells and in the HEV lumen. Finally, intracutaneous injections of ELC in *plt/plt* mice restored T cell homing to the draining lymph nodes. Altogether, our data showed that ELC is likely to participate in CCR7-mediated triggering of lymphocyte arrest in HEVs.

Materials and Methods

In Situ Hybridization. A 434-bp, digoxigenin (DIG)-labeled riboprobe was generated from the coding region of human ELC with a DIG RNA labeling kit according to the manufacturer's directions (Boehringer Mannheim). All steps were performed at room temperature unless otherwise noted. Frozen sections (8 μm) from tissue specimens embedded in OCT (TissueTek) were fixed in 4% paraformaldehyde/diethylpyrocarbonate (DEPC)-treated PBS (15 min) and subsequently washed twice (15 min each) in PBS containing 0.1% active DEPC (Sigma-Aldrich). After 15-min equilibration in 5× SSC, sections were prehybridized (2 h, 59°C) in a solution of 50% formamide, 5× SSC, 50 μg/ml yeast tRNA, 100 μg/ml heparin, 1× Denhardt's solution, 0.1% Tween 20, 0.1% CHAPS, and 5 mM EDTA. Sections were subsequently hybridized overnight at 59°C with 500 ng/ml of riboprobe in hybridization solution. A high stringency wash was performed in the following sequence: 2× SSC (30 min), 2× SSC (1 h, 65°C), and 0.1× SSC (1 h, 65°C). Sections were then equilibrated in buffer 1 (100 mM Tris-HCl, 150 mM NaCl, pH 7.5) for 15 min, incubated (2 h) with alkaline phosphatase–conjugated sheep anti-DIG (1:5,000; Boehringer Mannheim) and 0.5% Boehringer Blocking Agent dissolved in buffer 1, and subsequently given a wash in two changes of buffer 1 (15 min each). Sections were next equilibrated in the substrate buffer (100 mM Tris-HCl, 150 mM NaCl, 50 mM MgCl₂, pH 9.5) for 5 min, and finally developed overnight in substrate buffer containing nitroblue tetrazolium chloride and 5-bromo-4-chloro-3-indolyl-phosphate (Boehringer Mannheim) according to the manufacturer's instructions.

Immunohistochemistry. Immunostaining on cryosections (8 μm) from surgical specimens of fresh palatine tonsils (*n* = 4) and

Peyer's patches (*n* = 2) was performed as described (22). In brief, acetone-fixed sections were first incubated with a mixture of mAb MECA-79 (rat IgM, 1:30; courtesy of E.C. Butcher, Stanford University Medical School, Stanford, CA) and MAB361 (mouse IgG2ᵦ, 0.3 μg/ml; R&D Systems) against human ELC, followed by a mixture of Alexa Fluor 488 (Molecular Probes) conjugated goat anti–mouse IgG2ᵦ (1.5 μg/ml; Southern Biotechnology Associates, Inc.) and Cy3-conjugated goat anti–rat Ig (1:1,000; Jackson ImmunoResearch Laboratories). In another protocol, mAb LS134 (mouse IgG1, 5 μg/ml; LeukoSite) or AF361 (affinity-purified goat IgG, 5 μg/ml; R&D Systems) against human ELC was followed by Cy3-conjugated goat anti–mouse IgG1 (1:2,000; Southern Biotechnology Associates, Inc.) or Alexa Fluor 488–conjugated donkey anti–goat IgG (1:1,000; Molecular Probes), respectively. Negative controls were tissue sections incubated with irrelevant isotype- and concentration-matched mAbs.

Electron Microscopy. Immunoelectron microscopy was performed on sections of palatine tonsils (*n* = 3) as detailed elsewhere (22). In brief, tissue specimens were prefixed in 1% paraformaldehyde, and putative HEV-rich areas were cut into rectangular strips (2 × 2 × 5 mm), followed by immersion in 1% paraformaldehyde and 0.5% glutaraldehyde, dehydration in ethanol with progressive lowering of temperature to −20°C, and embedding in Unicryl (BioCell). Ultrathin sections were cut and mounted on formvar-coated nickel grids (Agar Scientific).

Sections were incubated with affinity-purified goat antibodies against human ELC (5 μg/ml; R&D Systems), followed by biotinylated rabbit anti-goat (1:100; Zymed Laboratories) and finally by 5-nm gold-conjugated streptavidin (1:40; Amersham Pharmacia Biotech). Sections were silver enhanced and contrasted with uranyl acetate and lead citrate. Control sections were incubated with concentration-matched normal goat IgG.

Autoradiography. To obtain functional information, HEV-rich tonsil specimens (5 × 5 × 5 mm) from two patients in separate experiments (each in triplicate) were incubated for 60 or 120 min at 37°C in RPMI/0.1% BSA (Life Technologies) containing 2.2 nM/12.5 μCi ^{125}I–ELC (NEN Life Science Products). For displacement binding experiments, 220 nM unlabeled ELC (R&D Systems) was added. The specimens were then washed three times for 5 min in PBS, fixed in 4% PFA at 4°C overnight, and finally snap frozen in OCT. In another set of experiments, 2.5 or 9 ng of ^{125}I–ELC (250 μCi/μg) or ^{125}I–MIP-1α (275 μCi/μg) (both from NEN Life Science Products) in PBS was injected into the hind and front footpads of 12-wk-old BALB/c mice (three mice per chemokine). After 90 min, the draining and contralateral popliteal and axillary lymph nodes were harvested and processed for autoradiography as described for the tonsillar specimens.

Cryosections (15 μm) of all tissue specimens were air dried overnight, and the localization of bound radioactive chemokine was revealed by autoradiography with Ilford K5 emulsion developed with D-19 developer (Eastman Kodak Co.) after 3–8 d of exposure at 4°C.

Lymphocyte Homing Assays. Donor T cells from mice expressing green fluorescent protein (GFP) under control of the murine CD4 promoter and proximal enhancer (T–GFP) (23) were prepared as described (9). In brief, lymph nodes were removed and passed through a 70-μm sterile nylon mesh (Corning). The resulting single-cell suspension was washed twice and resuspended at 10⁸ cells/ml in HBSS containing 1% FCS and 15 mM Hepes. Recipient *plt/plt* mice were anesthetized with ketamine/xylaxine and received an intracutaneous injection of recombinant murine

(rm)SLC or rmELC (2.5 nmol; R&D Systems; two mice per chemokine) unilaterally in the flank. The contralateral flank was injected with vehicle (50 μl PBS). After 10 min, 5×10^7 T–GFP lymphocytes were injected via the tail vein, and the mice were left to recover for 90 min. Thereafter, a blood sample was taken and the mice were killed. The ipsilateral subiliac lymph node, as well as the contralateral subiliac and brachial lymph nodes, were removed and digested with collagenase type II (Worthington Biochemical). The resulting single-cell suspension was analyzed by flow cytometry (FACScan™; Becton Dickinson) to determine the percentage of GFP+ T cells in each sample. To determine the total number of lymphocytes homing to each lymph node, a known number of PK26-labeled microspheres (Sigma-Aldrich) was added to each sample. For comparison of recruited T–GFP cells between the ipsilateral and contralateral lymph nodes, the paired Student's *t* test was used.
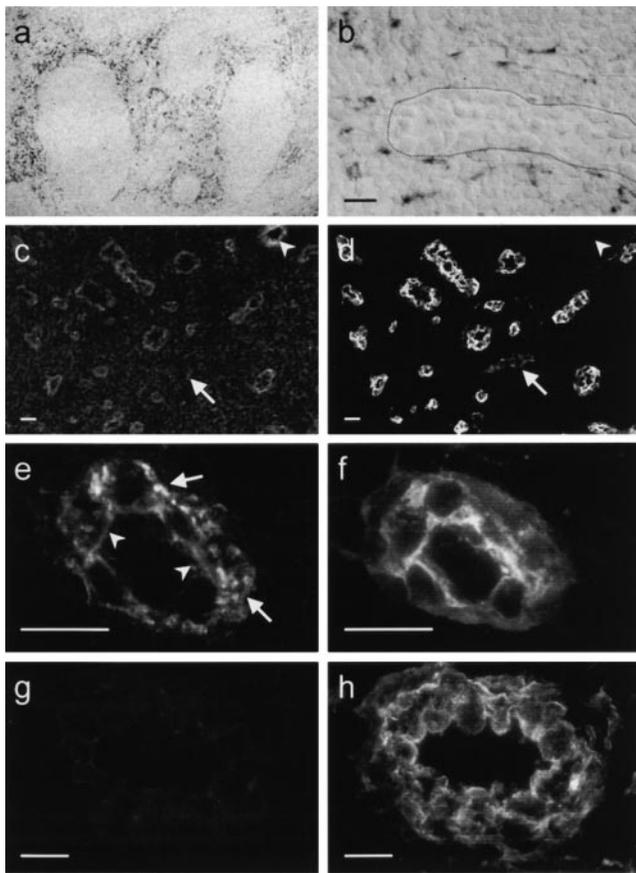
Results

ELC mRNA Is Expressed in the T Cell Zone of Human Tonsils but Not in HEVs. By means of mRNA hybridization analysis in situ, we confirmed and extended the findings reported by Dieu et al. (20) that ELC is expressed by nonendothelial cells in the T cell zone of human tonsils. Strikingly, the ELC antisense probe hybridized to spindle-shaped cells in the T zone (Fig. 1 a), as well as to perivascular cells intimately associated with the HEV basement membrane (Fig. 1 b), whereas no hybridization was observed in endothelial cells. Also, we found no ELC transcripts in B cell follicles or other areas outside the T cell zone. Hybridization with a sense probe gave no signal (not shown).

ELC Protein Is Found in Tonsillar HEVs and Perivascular Cells. Two-color immunofluorescence staining for ELC (Fig. 1 c) revealed a prominent labeling of 50–90% (range of four separate specimens) of MECA-79+ tonsil HEVs (Fig. 1 d). Furthermore, ELC labeling was not restricted to HEVs, as MECA-79− vessels in the T cell zone also contained chemokine (Fig. 1, c and d, arrowheads).
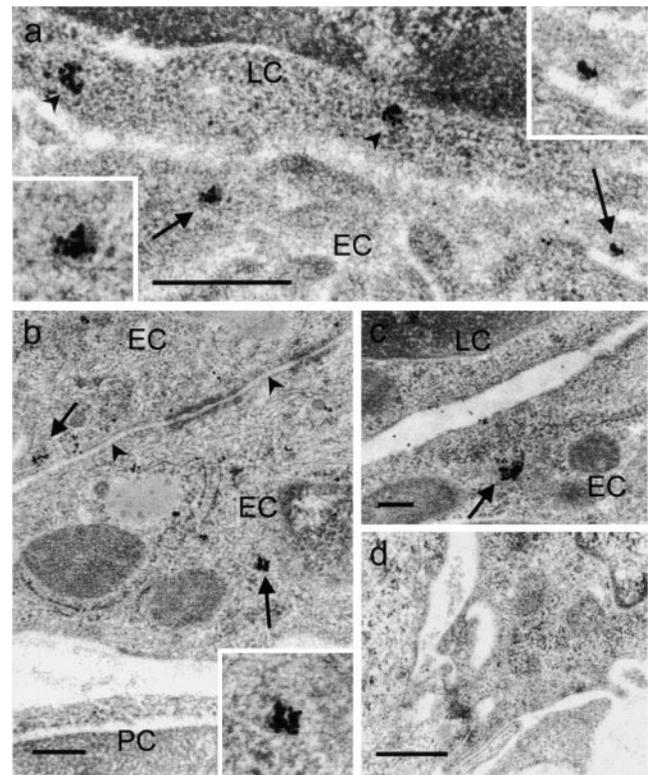

Figure 1. ELC protein is accumulated within HEVs, whereas ELC transcripts are found perivascularly. In situ hybridization with an RNA probe complementary to ELC mRNA. (a) Overview of tonsillar section showing positive cells (black) confined to T cell areas. (b) Higher magnification shows strong signals from perivascular cells partly surrounding the HEV (border delineated), whereas endothelial cells are negative. Single exposures of two-color immunofluorescence staining identifying ELC by means of MAB361 (c and e) and HEVs by means of mAb MECA-79 (d, f, and h). Most MECA79+ HEVs contain ELC, whereas MECA-79+ELC− vessels are also seen (c and d, arrows). MECA-79−ELC+ vessels are also found in the T cell zone (c and d, arrowheads). (e) HEV-associated ELC staining is distinctly luminal (arrowheads) and remarkably granular intracellularly (arrows), in contrast to the MECA-79 antigen distribution (f). Staining with an irrelevant control mAb (g) produces no signal together with MECA-79 (h). Scale bars: b and e–h, 15 μm; c and d, 25 μm.

Figure 2. ELC protein is found in cytoplasmic vesicles of HEVs and at the HEV–lymphocyte interface. Silver-enhanced immunogold staining with goat anti–human ELC on sections of Unicryl-embedded tonsillar tissue. (a) Electron micrograph of interface between an HEV cell and lymphocyte shows vesicle-associated gold particles near the luminal plasma membrane of endothelial cells (arrows and high magnification insets). Note also membrane-proximal cytoplasmic vesicles of adjacent lymphocyte (arrowheads). (b and c) ELC labeling in intracellular vesicles (arrows and high magnification inset). Note absence of markers in the interendothelial cleft (b, arrowheads). (d) Staining with irrelevant control antibody. EC, endothelial cell; LC, lymphocyte; PC, pericyte. Scale bars: a and d, 500 nm; b and c, 200 nm.

Higher magnification of MECA-79^{+} HEVs (Fig. 1 f) usually revealed a distinct luminal ELC staining as well as a remarkably granular intracellular pattern (Fig. 1 e). No labeling was observed with an irrelevant mouse control mAb (Fig. 1 g). Immunostaining for ELC with another mAb, or with a goat polyclonal antibody, produced similar staining patterns (data not shown). Furthermore, immunostained sections of Peyer's patches revealed ELC in intestinal HEVs (data not shown). ELC[+] granules were not colocalized with von Willebrand factor, a marker for regulated exocytosis in endothelial cells (data not shown).

ELC Is Present in Cytoplasmic Vesicles of HEV Cells and at HEV–Lymphocyte Interfaces. The subcellular localization of ELC was studied by immunoelectron microscopy. In this context, it should be emphasized that the tissue was fixed by exposure to low concentration of aldehydes and subsequent low-temperature Unicryl embedding, thus omitting postfixation in osmium tetroxide and heat polymerization. By this procedure, antigenic epitopes were well preserved, and fewer shrinkage artifacts were introduced, but at the cost of less distinct subcellular membranes. Therefore, intracellular vesicles could be identified primarily by means of focally concentrated immunolabeling. In sections of tonsillar tissue, we found distinct HEV-associated ELC labeling of intracellular vesicles in all parts of the cytoplasm, including the luminal regions (Fig. 2, a–c, arrows). These vesicles were of variable diameter and consistent with vesicular transport. Notably, gold particles were not observed in the interendothelial clefts (Fig. 2 b, arrowheads), thus making paracellular transport of ELC quite unlikely. Furthermore, ELC was found in membrane-proximal vesicles of adjacent lymphocytes (Fig. 2 a, arrowheads), probably reflecting receptor binding and subsequent internalization of the ligand–receptor complex (24). Sections incubated with concentration-matched irrelevant goat IgG showed no staining (Fig. 2 d).

HEVs Possess Binding Sites for ELC. To test whether HEV cells have a functional capacity for ELC binding in situ, we prepared tonsillar tissue specimens for organ culture with addition of ^{125}I–ELC and subsequent autoradiography. We restricted our analysis to tissue areas ~1.5 mm from the edges of the sections to avoid sampling errors due to diffusion of the incubation medium. After 60 min of incubation, radioactive signals were predominantly associated with HEVs (Fig. 3 a) and their lumina (Fig. 3 b), whereas the surrounding tissue was only weakly labeled. Notably, flat-walled vessels of all calibers failed to emit signals above background levels (Fig. 3 c and data not shown). This argues against general vascular perfusion and rapid filling of ^{125}I–ELC-containing buffer in larger lumen blood vessels such as HEVs or that it is the meniscus of emulsion that forms at the edge of tissue that gives rise to the grains. Addition of 100-fold excess of unlabeled ELC substantially reduced the radioactive signals (Fig. 3 d).

ELC Injected into Footpads of Mice Accumulates in HEVs of Draining Lymph Nodes. To directly assess whether HEV cells have a functional capacity for basolateral ELC uptake and luminal presentation in vivo, we determined the fate of footpad-injected ^{125}I–ELC in BALB/c mice by autoradiography. After 90 min, injected ELC was readily detected in afferent lymphatics (Fig. 4 a, arrow), as well as in the subcapsular sinus (arrowheads) of draining popliteal and axillary lymph nodes. As shown in Fig. 4, b–f, examination of the lymph node stroma revealed ELC signals predominantly in lymphatic sinus of the paracortical T cell zone (arrowheads) and associated with HEVs (arrows). Radiolabeling was seen both inside HEV cells and on their luminal surfaces. Injected MIP-1α was also targeted to the subcapsular region of draining lymph nodes (not shown) but was preferentially sequestered within the cortical B cell zone and was not found in HEV cells of the T cell zone (Fig. 4 g). However, some HEVs near the follicular mantle zones contained weak radiolabel (not shown). Endothelial cells in contralateral lymph nodes from all animals contained no radiolabel (Fig. 4 h and data not shown), ruling out systemic delivery of chemokines in our experiments.
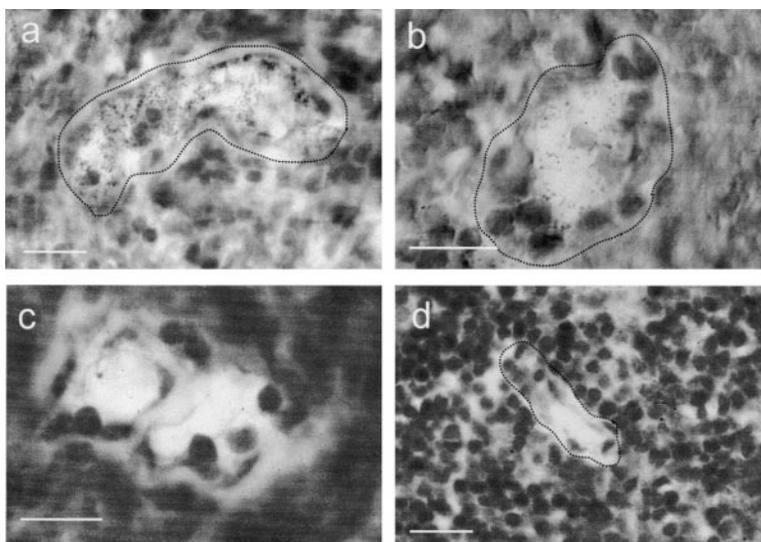

Figure 3. HEVs possess binding sites for ELC. Autoradiography of tissue sections made after tonsillar organ culture with radioiodinated ELC. (a and b) Strong signals are predominately associated with HEV cells and the HEV lumen. In contrast, flat-walled vessels (c) show no signal. (d) Addition of excess cold ELC abolishes HEV-associated signals. Scale bars: 25 μm.
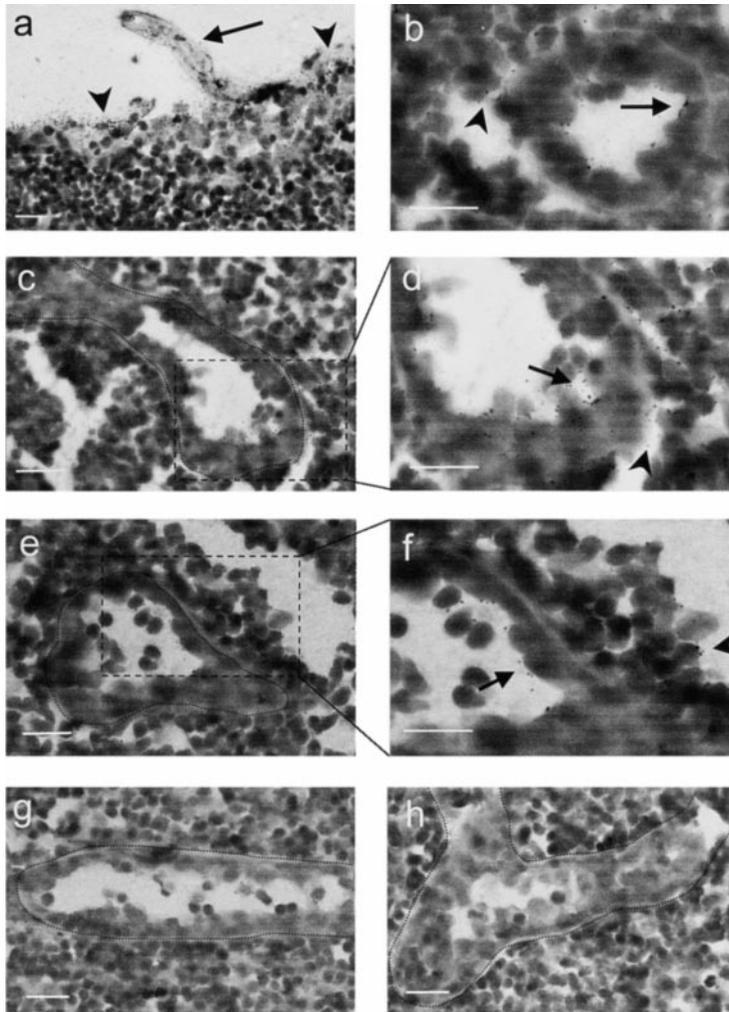
Figure 4. ELC injected into mice footpads is taken up by HEVs and presented at their luminal surfaces. ^{125}I–ELC injected into BALB/c mice is detected by autoradiography in the afferent lymphatics (a, arrow) as well as in the subcapsular sinus (arrowheads) of draining lymph nodes after 90 min. In the T zone, ELC signals are predominately found in the HEVs (b, arrow) and lymphatic sinus (arrowheads). Higher magnification of areas outlined in c and e reveals radiolabel both inside HEV cells and on their luminal surfaces (d and f, arrows), as well as in the surrounding sinus (arrowheads). Injected ^{125}I–MIP-1α is preferentially sequestered within the B zone, but HEV cells in the T zone are not labeled (g). Endothelial cells in contralateral lymph nodes contain no radiolabel (ELC-injected mouse shown in h). Scale bars: 25 μm.

Intracutaneously Injected ELC Reconstitutes T Cell Homing to plt/plt Lymph Nodes. To directly test whether ELC has the capacity to mediate T cell homing to lymph nodes, *plt/plt* mice received intracutaneous injections of either ELC or SLC (2.5 nmol of each) unilaterally in the flank skin, followed by intravenous transfer of fluorescent T cells (T–GFP) (23). After 90 min, we found that significantly more T–GFP cells homed to lymph nodes draining the ELC injection site compared with the contralateral lymph nodes. Furthermore, at the dose tested, intracutaneously injected ELC recruited T–GFP cells to lymph nodes as efficiently as SLC (Fig. 5 a). All mice had similar circulating level of T–GFP cells (Fig. 5 b).

Discussion

A role for chemokines in lymphocyte adhesion triggering has gained direct experimental support only recently (4, 9, 25). Solid evidence to this end comes from experiments in *plt/plt* mice that have reduced numbers of T cells in peripheral lymph nodes (11) and lack SLC expressed in HEVs (9, 10, 12, 13). In fact, normal T cells injected into *plt/plt* mice interact with HEVs by rolling at normal rates but fail to en-

gage in trigger-dependent adhesion (9, 10). Although data generated in *plt/plt* mutants and normal mice suggest a crucial role of SLC in the recruitment of T cells, the interpretation of these experiments is complicated by several issues. First, novel data show that *plt/plt* mice not only lack SLC but also ELC protein in their peripheral lymphoid organs. The single functional ELC gene is deleted in these mice, and the transcripts detected in previous studies stem from one or more nonfunctional pseudogenes (17, 18). Hence, *plt/plt* mice are deficient in both CCR7 ligands in their lymphoid tissue. Second, CCR7 was desensitized by pretreatment with either SLC or ELC before injection, thereby corroborating a role for CCR7 but not identifying the involvement of either ligand alone. Third, despite a proposed role for the elongated, basic COOH terminus of SLC in enhanced tethering to proteoglycans in the HEV lumen (9), other chemokines (IL-8 and RANTES (regulated upon activation, normal T cell expressed and secreted)/CCL5; see below) can also be presented at the luminal face of venules (21), indicating that this elongation is not an absolute requirement for luminal chemokine retention. Therefore, in light of our study, ELC and SLC may be equally important triggers of CCR7-mediated adhesion, and the dissection of
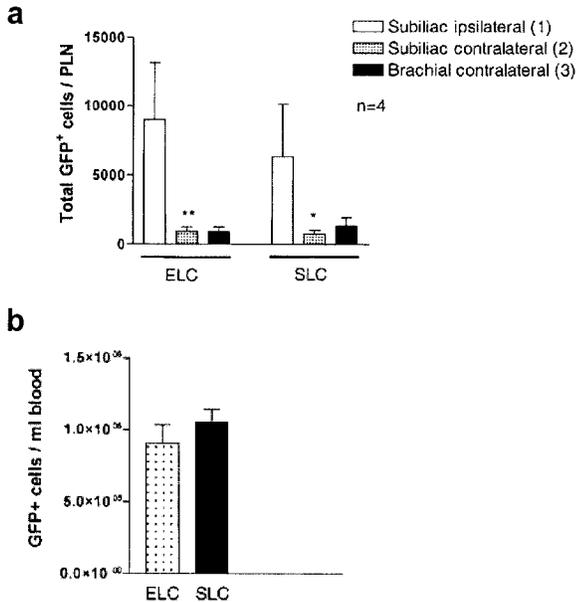
Figure 5. Intracutaneously injected ELC reconstitutes T cell homing to lymph nodes in *plt/plt* mice. *plt/plt* mice received intracutaneous injections of ELC, SLC (2.5 nmol), or PBS vehicle (50 μl) in the flank skin, followed by transfer of green fluorescent T cells (T–GFP) through the tail vein. (a) Total number of T–GFP cells homed to lymph nodes after 90 min. Significantly more cells homed to the ipsilateral than the contralateral lymph nodes. (b) There was no difference in the circulating level of T–GFP cells (*$P < 0.005$, **$P < 0.003$). Data are shown as mean ± SEM. $n = 4$ animals per chemokine.

their relative importance awaits future in vivo studies and the use of blocking mAbs to either chemokine.

Our data demonstrate convincingly that ELC generated in the perivascular interstitium was translocated by HEVs to their luminal faces. Although transcription of ELC was restricted to cells in the perivascular stroma, ELC protein was found in cytoplasmic vesicles of HEV cells and associated with their surface membranes. ELC staining on tonsillar HEVs has recently also been reported by others (24). Furthermore, radiolabeled ELC added to our tonsillar organ cultures was almost exclusively localized to HEVs, thus showing that HEVs possess binding sites for ELC. This might be constituted by the very prominent and acidic glycocalyx found on HEV cells and endothelial cells of other postcapillary venules (26), which could bind the basic ELC. Moreover, lymph-borne ELC delivered to the abluminal surfaces of HEVs was translocated and apparently presented at the HEV lumen. Finally, exogenous ELC restored T cell homing to *plt/plt* lymph nodes in vivo at least as efficiently as SLC.

Taken together, our study lends strong support to the proposed mechanism of abluminal-to-luminal transcytosis of chemokines in postcapillary venules (21). Chemokine transcytosis in HEV cells may not be restricted to ELC, because intradermally injected SLC is rapidly translocated to the surfaces of HEVs in draining lymph nodes (9). Furthermore, mast cell–derived MIP-1β (CCL4) is known to be presented within HEV in inflamed lymph nodes (27). Al-

though the molecular mechanism for chemokine uptake and transcytosis in endothelial cells remains unclear, the Duffy antigen/receptor of chemokines (DARC) has been implicated in the endothelial binding and transcytosis of IL-8 and RANTES (21). Moreover, DARC is strongly and quite specifically expressed by tonsillar HEV cells (22). However, we were unable to detect affinity of ELC to two different DARC transfectants in vitro (unpublished data) and hypothesize that ELC might therefore utilize other molecules with chemokine-binding properties. Possible candidates could include sulfated glycosaminoglycans such as heparan sulfate, which appears to be important for the interaction of IL-8 with endothelial cells (21).

A mechanism for delivery of interstitial chemokines to the abluminal surfaces of HEVs has been directly addressed only recently (28). Small soluble molecules (including chemokines) were shown to traverse the lymph node cortex via the reticular network system of collagen fibers, a protein meshwork extending from the subcapsular sinus to ensheath the HEVs (29). Indeed, Gretz et al. (28) found lymph borne MIP-1α (CCL3) localized to this reticular network and around HEVs 5–30 min after footpad injections. Our observation of follicle-associated MIP-1α could be explained by the fact that we sampled after 90 min. We also found ELC labeling associated with collagen fibers in the tonsillar stroma by immunoelectron microscopy, in a pattern possibly corresponding to this conduit system (unpublished observations).

In conclusion, this study provides strong evidence that ELC can be made available to rolling lymphocytes in HEVs by specific endothelial uptake and transcytosis. Therefore, we suggest that the relative importance of ELC versus SLC should be reevaluated.

References

1. von Andrian, U.H., and C.R. Mackay. 2000. T-cell function and migration. Two sides of the same coin. *N. Engl. J. Med.* 343:1020–1034.
2. Butcher, E.C., and L.J. Picker. 1996. Lymphocyte homing and homeostasis. *Science.* 272:60–66.
3. Girard, J.P., and T.A. Springer. 1995. High endothelial venules (HEVs): specialized endothelium for lymphocyte mi-

gration. *Immunol. Today.* 16:449–457.

4. Campbell, J.J., J. Hedrick, A. Zlotnik, M.A. Siani, D.A. Thompson, and E.C. Butcher. 1998. Chemokines and the arrest of lymphocytes rolling under flow conditions. *Science.* 279:381–384.

5. Cyster, J.G. 1999. Chemokines and cell migration in secondary lymphoid organs. *Science.* 286:2098–2102.

6. Zlotnik, A., and O. Yoshie. 2000. Chemokines: a new classification system and their role in immunity. *Immunity.* 12:121–127.

7. Campbell, J.J., and E.C. Butcher. 2000. Chemokines in tissue-specific and microenvironment-specific lymphocyte homing. *Curr. Opin. Immunol.* 12:336–341.

8. Gunn, M.D., K. Tangemann, C. Tam, J.G. Cyster, S.D. Rosen, and L.T. Williams. 1998. A chemokine expressed in lymphoid high endothelial venules promotes the adhesion and chemotaxis of naive T lymphocytes. *Proc. Natl. Acad. Sci. USA.* 95:258–263.

9. Stein, J.V., A. Rot, Y. Luo, M. Narasimhaswamy, H. Nakano, M.D. Gunn, A. Matsuzawa, E.J. Quackenbush, M.E. Dorf, and U.H. von Andrian. 2000. The CC chemokine thymus-derived chemotactic agent 4 (TCA-4, secondary lymphoid tissue chemokine, 6Ckine, exodus-2) triggers lymphocyte function-associated antigen 1-mediated arrest of rolling T lymphocytes in peripheral lymph node high endothelial venules. *J. Exp. Med.* 191:61–75.

10. Warnock, R.A., J.J. Campbell, M.E. Dorf, A. Matsuzawa, L.M. McEvoy, and E.C. Butcher. 2000. The role of chemokines in the microenvironmental control of T versus B cell arrest in Peyer's patch high endothelial venules. *J. Exp. Med.* 191:77–88.

11. Nakano, H., T. Tamura, T. Yoshimoto, H. Yagita, M. Miyasaka, E.C. Butcher, H. Nariuchi, T. Kakiuchi, and A. Matsuzawa. 1997. Genetic defect in T lymphocyte-specific homing into peripheral lymph nodes. *Eur. J. Immunol.* 27:215–221.

12. Gunn, M.D., S. Kyuwa, C. Tam, T. Kakiuchi, A. Matsuzawa, L.T. Williams, and H. Nakano. 1999. Mice lacking expression of secondary lymphoid organ chemokine have defects in lymphocyte homing and dendritic cell localization. *J. Exp. Med.* 189:451–460.

13. Vassileva, G., H. Soto, A. Zlotnik, H. Nakano, T. Kakiuchi, J.A. Hedrick, and S.A. Lira. 1999. The reduced expression of 6Ckine in the plt mouse results from the deletion of one of two 6Ckine genes. *J. Exp. Med.* 190:1183–1188.

14. Forster, R., A. Schubel, D. Breitfeld, E. Kremmer, I. Renner-Muller, E. Wolf, and M. Lipp. 1999. CCR7 coordinates the primary immune response by establishing functional microenvironments in secondary lymphoid organs. *Cell.* 99:23–33.

15. Yoshida, R., T. Imai, K. Hieshima, J. Kusuda, M. Baba, M. Kitaura, M. Nishimura, M. Kakizaki, H. Nomiyama, and O. Yoshie. 1997. Molecular cloning of a novel human CC chemokine EBI1-ligand chemokine that is a specific functional ligand for EBI1, CCR7. *J. Biol. Chem.* 272:13803–13809.

16. Campbell, J.J., E.P. Bowman, K. Murphy, K.R. Youngman, M.A. Siani, D.A. Thompson, L.J. Wu, A. Zlotnik, and E.C. Butcher. 1998. 6-C-kine (SLC), a lymphocyte adhesion-triggering chemokine expressed by high endothelium, is an agonist for the MIP-3 beta receptor CCR7. *J. Cell Biol.* 141: 1053–1059.

17. Luther, S.A., H.L. Tang, P.L. Hyman, A.G. Farr, and J.G. Cyster. 2000. Coexpression of the chemokines ELC and SLC by T zone stromal cells and deletion of the ELC gene in the plt/plt mouse. *Proc. Natl. Acad. Sci. USA.* 97:12694–12699.

18. Nakano, H., and M.D. Gunn. 2001. Gene duplications at the chemokine locus on mouse chromosome 4: multiple strain-specific haplotypes and the deletion of secondary lymphoid-organ chemokine and EBI-1 ligand chemokine genes in the plt mutation. *J. Immunol.* 166:361–369.

19. Ngo, V.N., H.L. Tang, and J.G. Cyster. 1998. Epstein-Barr virus-induced molecule 1 ligand chemokine is expressed by dendritic cells in lymphoid tissues and strongly attracts naive T cells and activated B cells. *J. Exp. Med.* 188:181–191.

20. Dieu, M.C., B. Vanbervliet, A. Vicari, J.M. Bridon, E. Oldham, S. Ait-Yahia, F. Briere, A. Zlotnik, S. Lebecque, and C. Caux. 1998. Selective recruitment of immature and mature dendritic cells by distinct chemokines expressed in different anatomic sites. *J. Exp. Med.* 188:373–386.

21. Middleton, J., S. Neil, J. Wintle, I. Clark-Lewis, H. Moore, C. Lam, M. Auer, E. Hub, and A. Rot. 1997. Transcytosis and surface presentation of IL-8 by venular endothelial cells. *Cell.* 91:385–395.

22. Girard, J.P., E.S. Baekkevold, T. Yamanaka, G. Haraldsen, P. Brandtzaeg, and F. Amalric. 1999. Heterogeneity of endothelial cells: the specialized phenotype of human high endothelial venules characterized by suppression subtractive hybridization. *Am. J. Pathol.* 155:2043–2055.

23. Manjunath, N., P. Shankar, B. Stockton, P.D. Dubey, J. Lieberman, and U.H. von Andrian. 1999. A transgenic mouse model to analyze CD8(+) effector T cell differentiation in vivo. *Proc. Natl. Acad. Sci. USA.* 96:13932–13937.

24. Breitfeld, D., L. Ohl, E. Kremmer, J. Ellwart, F. Sallusto, M. Lipp, and R. Forster. 2000. Follicular B helper T cells express CXC chemokine receptor 5, localize to B cell follicles, and support immunoglobulin production. *J. Exp. Med.* 192: 1545–1551.

25. Warnock, R.A., S. Askari, E.C. Butcher, and U.H. von Andrian. 1998. Molecular mechanisms of lymphocyte homing to peripheral lymph nodes. *J. Exp. Med.* 187:205–216.

26. Anderson, A.O., and S. Shaw. 1993. T cell adhesion to endothelium: the FRC conduit system and other anatomic and molecular features which facilitate the adhesion cascade in lymph node. *Semin. Immunol.* 5:271–282.

27. Tedla, N., H.W. Wang, H.P. McNeil, N. Di Girolamo, T. Hampartzoumian, D. Wakefield, and A. Lloyd. 1998. Regulation of T lymphocyte trafficking into lymph nodes during an immune response by the chemokines macrophage inflammatory protein (MIP)-1 alpha and MIP-1 beta. *J. Immunol.* 161:5663–5672.

28. Gretz, J.E., C.C. Norbury, A.O. Anderson, A.E. Proudfoot, and S. Shaw. 2000. Lymph-borne chemokines and other low molecular weight molecules reach high endothelial venules via specialized conduits while a functional barrier limits access to the lymphocyte microenvironments in lymph node cortex. *J. Exp. Med.* 192:1425–1439.

29. Gretz, J.E., E.P. Kaldjian, A.O. Anderson, and S. Shaw. 1996. Sophisticated strategies for information encounter in the lymph node. The reticular network as a conduit of soluble information and a highway for cell traffic. *J. Immunol.* 157:495–499.